Optical shielding of cold collisions

Kalle-Antti Suominen, Murray J. Holland,* and Keith Burnett
Clarendon Laboratory, Department of Physics, University of Oxford, Parks Road, Oxford OX1 3PU, United Kingdom

Paul Julienne
Molecular Physics Division, National Institute for Standards and Technology, Gaithersburg, Maryland 20899-0001
(Received 12 July 1994; revised manuscript received 22 September 1994)

Inelastic collision rates between two very cold ground-state atoms can be strongly decreased by using an optical shielding laser to repel the colliding atoms at very large internuclear separation so that they never get close to each other. This can be achieved by using a sufficiently intense laser to excite a repulsive state of the quasimolecule formed by the two colliding atoms. We study a simple two-state model and compare the predictions of fully quantum-mechanical close coupling and time-dependent wave packet methods with semiclassical approximations based on the concept of a Landau-Zener curve crossing of field-dressed states. The effect of spontaneous emission in the excited state is treated by the Monte Carlo wave-function method. Calculations are given for a model sodium system at 250 μK. Strong optical shielding, without significant heating due to the quasimolecular excitation, can be achieved at relatively modest laser power. We find that Landau-Zener models give near quantitative agreement with the fully quantum calculations in spite of the extremely low temperature.

PACS number(s): 32.80.Pj, 42.50.Vk, 03.65.−w

I. INTRODUCTION

Studies of cold collisions of neutral atoms with $T \ll 1$ mK in the presence of light fields have recently become important because of the advances in laser cooling and trapping [1]. Such collisions can lead to the loss of atoms from a magneto-optical trap [2–9] or a far-off-resonance optical trap [10,11]. Ground-state collisions that change the hyperfine state can also lead to the loss of magnetically trapped atoms [12–14]. The densities that can be obtained currently in atom traps are large enough for collisions to have an important role. They can, for instance, strongly diminish the possibilities to prepare and observe a Bose-Einstein condensate of trapped and cooled atoms [15]. The suppression of inelastic collisional effects is, therefore, a necessary condition for reaching low temperatures and high densities simultaneously. One method for producing such suppression is to prevent the colliding atoms from reaching the relatively small interatomic distances where the inelastic processes take place. This can be achieved by using optical shielding, i.e., laser-induced excitation of the collisional diatomic quasimolecule to a repulsive potential curve, thereby forcing the colliding atoms to separate. The effect has very recently been studied experimentally by several groups [16–19]. Marcassa *et al.* [16] have reported suppression of probe laser absorption by adding a blue-detuned laser to deflect the approaching atoms, and we presented accompanying quantum and semiclassical calculations to account for the effect. Bali *et al.* [17] observed the enhancement of trap loss by exciting a repulsive state and gave a Landau-Zener curve crossing model to explain their observations. Tan *et al.* [18] obtained preliminary evidence of shielding of ground-state hyperfine changing collisions and used semiclassical optical Bloch equation calculations to study the magnitude of the expected effect. Recent experimental studies have clearly demonstrated the existence of optical shielding of Penning ionization collisions of metastable xenon [19] and krypton [20].

In this article we present a detailed theoretical study of optical shielding and an extension of the short discussion provided in Ref. [16]. Our fully quantum-mechanical analysis includes the effect of light shifts, saturation, and population recycling due to an intense light field, and the effect of spontaneous decay during the slow collision. A robust conclusion of this analysis is the striking success of some simple Landau-Zener models, which agree rather well with the time-consuming and complicated quantum calculations. We consider only the case where the detuning from atomic resonance is large compared to the natural linewidth of the cooling transition. The choice of our model parameters was dictated by two considerations: (1) our initial motivation to show that optical shielding can have a role in interpreting ionization rates in two-color experiments, such as the one presented in Ref. [21] and (2) the desire to keep detuning fairly small (five linewidths in our model) so as to test the disruption of the shielding mechanism by spontaneous decay. However, we expect our results to represent most of the essential physics of the process and our conclusions to be generally applicable to other cases. The main simplifying assumptions of our collision model are that only one of the excited-states of the quasimolecule participate in the laser-induced processes and that spherically averaged Rabi coupling can be used. This two-state approach can be questioned, because both the alkali-atom and metastable rare-gas species, which are the main target of laser cooling and trapping, have extensive multi-

*Present address: JILA, University of Colorado, Boulder, CO 80309.

level molecular structure due to the high spin degeneracy. This is certainly true for sodium [22], which we have chosen as our study case. However, an adequate quantum-mechanical theoretical treatment of the collisions in the presence of a strong light field is simply impossible for the moment unless such a simplification is assumed, and some insight into the physics of shielding collisions is provided by the two-state models, as well as testable predictions. As demonstrated in Ref. [17], the multistate problem may in some cases be regarded as a group of independent two-state processes. The most important support for two-state shielding studies, however, comes from the experiments that have demonstrated the usefulness of the simple two-state Landau-Zener model [23,24] in the description of the observed data [16,17].

In Fig. 1(a) we show the basic system for optical shielding. The collision process is described in the time-dependent picture. As the two atoms approach each other the interatomic distance R diminishes and at the Condon point R_C the blue-detuned laser field becomes resonant with the transition from the ground state of the quasimolecule to one of the excited states, which is represented by a repulsive potential curve $U_e(R)$. In the absence of the laser field the undisturbed atoms reach the inner region of the collisional ground-state quasimolecule, where $R \ll R_C$ and various processes can take place. Examples of such inner region processes are probe laser absorption [11,16], inelastic hyperfine changing collisions due to spin-dipole or exchange interactions [13,14], or Penning ionization of rare-gas metastables [19,20]. However, with the blue-detuned laser we can transfer the quasimolecule to an excited state, as described schematically in Fig. 1(a). The repulsive potential slows the relative motion down and eventually the two atoms are reflected. Classically the reflection takes place at the turning point $R_{\rm tp}$ where the potential-energy difference $U_e(R_{\rm tp}) - U_e(R_C)$ equals $E^0_{\rm kin}$, the initial relative kinetic energy. Therefore, reaching the inner region is forbidden and the collision becomes shielded. Alternatively, we can say that the inner region inelastic processes are suppressed, which is the terminology adopted in Ref. [16]. We define the shielding measure P_S as a probability for the quasimolecule to reach the inner region on the initial ground-state channel. The probability of inner zone ground-state processes are decreased by this factor. For efficient shielding we need $P_S \ll 1$.

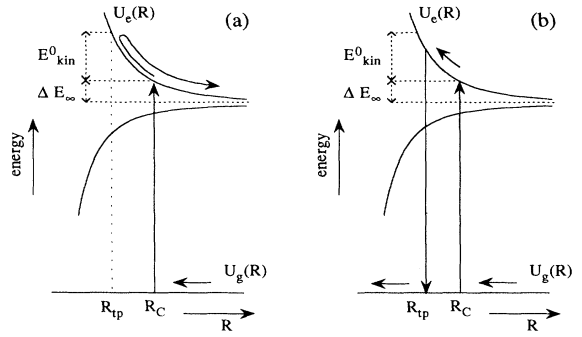

FIG. 1. The schematic model for optical shielding in a two-state system. The ground- and excited-state potential curves are $U_g(R)$ and $U_e(R)$, respectively. The external laser field brings these curves to resonance at the interatomic distance $R = R_C$. In the absence of weak decay we have situation (a) the system approaching from large R is excited at R_C, then slows down and is eventually reflected on the excited state at the turning point $R_{\rm tp}$. It can then remain in this state or return to ground state as it passes R_C again. $E^0_{\rm kin}$ marks the initial kinetic energy of the system, and E_∞ is the asymptotic increase in kinetic energy. In (b) we show how spontaneous decay can affect the process: the system may decay back to ground state before it reaches $R_{\rm tp}$ and can then continue its motion to the inner region located at $R \ll R_C$.

The nature of the shielding process, however, depends on the time scale for spontaneous decay. If the decay is weak and we can ignore it, then the shielding model of Fig. 1(a) is valid. When the time it takes for the system to move on the excited state from R_C to $R_{\rm tp}$ is large compared to the average lifetime of the excited-state population, the efficiency of the shielding process may be reduced. The excited-state population can decay back to the ground state before it has reached $R_{\rm tp}$, as demonstrated in Fig. 1(b). Even if the approaching atoms have lost some kinetic energy during the stay on the excited state they can still possess negative relative momentum $p = \mu(dR/dt)$ (negative for approaching atoms, positive for reflected ones; μ is the reduced mass of the two-atom system) and, therefore, reach the inner region. However, for suitably strong fields studies of radiative heating [25,26] and small-distance excited-state survival [27] have shown that re-excitation of the decayed population (recycling) mixes this simple picture, and we show that the shielding is preserved by this recycling mechanism, at least for our study case, and this is in fact predicted by a simple semiclassical model.

It should be noted that the shielding process itself has an inelastic character. After the atoms have been reflected on the excited-state the quasimolecule re-enters the resonance region at R_C and stimulated population transfer back to the ground state can then take place. However, some population may survive on the excited state to large $R \gg R_C$. The asymptotic potential-energy difference $E_\infty \equiv U_e(R_C) - U_e(R \to \infty)$ becomes an increase in the final kinetic energy: $E^f_{\rm kin} = E^0_{\rm kin} + E_\infty$; E_∞ is equal to $\hbar\Delta$, where Δ is the laser detuning from the atomic transition. Therefore, at large Δ notable survival on the excited state at $R \gg R_C$ can lead to trap loss, and at small Δ it contributes to the heating of the atomic cloud. In fact, the trap loss observed for rubidium in Ref. [17] arises from this process and serves as a measure of validity for the Landau-Zener approach to be discussed in Sec. II. In the presence of strong spontaneous decay the above picture for kinetic-energy exchange associated with the shielding becomes more complicated. The clear exchange of energy is then turned into a radiative process. One expects this process to create a final ground-state kinetic-energy distribution, which has a tail that extends from $E^0_{\rm kin}$ to $E^0_{\rm kin} + E_\infty$. In Sec. III we show that this is indeed the case.

A third aspect of the optical shielding is the role of the processes taking place in the inner region. We can

describe the problem with probability flux and scattering amplitudes. The incoming initial flux is affected by the shielding, which turns some part of the flux into an outgoing contribution. When some of the unshielded flux is reflected in the inner region and returns to the region $R \simeq R_C$, the interference between the two outgoing flux contributions can take place. This is because in the absence of strong spontaneous decay the contributions retain their phase coherence (unless it is totally destroyed in the inner region by some process). The interference affects the distribution of the outgoing flux between the ground and excited states at R_C. Generally such phase effects are expected to be wiped out in most experiments, but we shall give them some attention in Sec. II.

We use different methods for studying the optical shielding. In the absence of spontaneous decay we estimate the efficiency of the shielding process using the Landau-Zener model with classical trajectories. We shall discuss this semiclassical method and its limitations. Furthermore, we shall combine the Landau-Zener approach with exponential decay and recycling, and produce semiclassical models for the shielding measure P_S. A test of accuracy for the semiclassical methods is provided by time-independent quantum close-coupling calculations [28], time-dependent wave-packet dynamics simulations [29–31], and, in the case of spontaneous decay by the Monte Carlo wave-function technique [26,32,33].

This paper is organized as follows. In Sec. II we concentrate on situations where spontaneous decay is weak, i.e., practically absent. We present the basics for the quantal approaches in this limit. Then we describe the semiclassical Landau-Zener model and its validity conditions. The results from different methods are compared in order to verify these conditions. In Sec. III we determine the cases when spontaneous decay can be important with a study of time scales, and present extended semiclassical Landau-Zener models for the shielding measure P_S. We also show results from the Monte Carlo approach for P_S and for the shielding-induced radiative heating, and show how well the extended Landau-Zener models describe the strong decay case. In Sec. IV we discuss the implications of our results for optical shielding and cold collisions.

II. WEAK SPONTANEOUS DECAY

We call spontaneous decay weak when it can be ignored in calculations for the shielding measure. Then we can use the methods presented in this section. Our approach is mainly based on the time-dependent view, although some concepts of time-independent scattering theory are employed in interference studies (the quantum close-coupling method).

A. The quantum methods

In the full quantum description the probability to find the two colliding atoms at the relative interatomic distance R is given by the wave packet $P(R,t) = |\Psi(R,t)|^2$, where $\Psi(R,t)$ is simply the quantum-mechanical two-component state vector for the system. The ground- and excited-state components of this wave packet, $P_g(R,t) = |\Psi_g(R,t)|^2$ and $P_e(R,t) = |\Psi_e(R,t)|^2$, respectively, become after an integration over R the occupation probabilities, i.e., populations of these states. The dynamics of this wave packet is obtained by solving the time-dependent coupled Schrödinger equation for $\Psi(R,t)$,

$$i\hbar\frac{\partial\Psi(R,t)}{\partial t} = H(R)\Psi(R,t), \tag{1}$$

where the 2×2 Hamiltonian and the two-component state vector are

$$H(R) = \begin{pmatrix} T(R)+U_g(R) & \hbar\Omega \\ \hbar\Omega & T(R)+U_e(R) \end{pmatrix}, \tag{2}$$

$$\Psi(R,t) = \begin{pmatrix} \Psi_g(R,t) \\ \Psi_e(R,t) \end{pmatrix}. \tag{3}$$

Here $T(R)$ is the kinetic-energy operator and $U_g(R)$ and $U_e(R)$ are the ground- and excited-state potential curves, respectively. One should note that we have used the rotating wave approximation and shifted the excited state down in energy by one laser photon, $\hbar\omega$ (now included in U_e). This eliminates the oscillatory terms from the laser coupling and the Hamiltonian becomes time independent. Then the Schrödinger equation (1) is numerically more accessible. The shift in excited-state energy also transfers the problem into a picture where the resonance points appear as curve crossings. We show the shielding model in this picture in Fig. 2.

The complete quantum-mechanical problem should treat the three-dimensional aspects of the collision, accounting for the direction of laser polarization and the relative angular momentum of the two atoms. If molecular total angular momentum basis states, $|JM\alpha R\rangle, \alpha = g$ or e, are used for the two-channel wave function in Eq. (3), the radiative coupling matrix element $\hbar\Omega$ in Eq. (2) is [34]

$$\begin{aligned}\hbar\Omega &= \langle JMgR|\vec{E}_q\cdot\vec{d}|J'M'eR\rangle \\ &= (J1J'|MqM')\hbar\Omega_{ge}(JJ'R).\end{aligned} \tag{4}$$

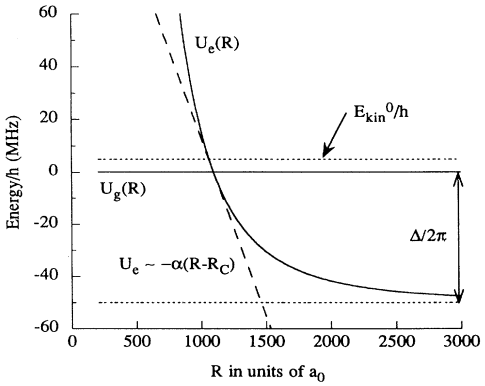

FIG. 2. The shielding model in the curve crossing picture. The notation is same as in Fig. 1. The tangent of the excited-state potential curve at R_C is shown as a dashed line.

Here $q = 0, \pm 1$ gives the polarization of the electric vector $\vec{E}_q$ of the light, M, M' are the projection quantum numbers on the space-fixed quantization axis, and the reduced Rabi matrix element $\Omega_{ge}(JJ'R)$ is proportional to $\sqrt{I}$, where I is the laser intensity. The specific relation is

$$\Omega_{ge}/2\pi = (17.35 \text{ MHz})\sqrt{I \text{ (W/cm}^2)}d_{ge}, \tag{5}$$

where I is the power in W/cm^2 and d_{ge} is the reduced transition dipole in atomic units of ea_0 (e = electron charge, $a_0 = 5.2918 \times 10^{-11}$ m). The second line of Eq. (4) follows from the Wigner-Eckart theorem. Complete quantum calculations must account for the breaking of spherical symmetry by the field (expressed by the fact that J and J' can differ by one unit) and the range of $\hbar\Omega$ due to the spread in $|M|$ between 0 and $\min(J, J')$ [34]. In the present model calculation we ignore the dependence of $\hbar\Omega$ on J, J', M, M', and assume that the Clebsh-Gordan coefficient in Eq. (4) can be replaced by $1/\sqrt{3}$, which is the square root of the spherical average of $(J1J'|MqM')^2$. This is a standard approximation for describing collisions in a strong radiation field [34,35]. The use of a root-mean-square approximation for the Rabi coupling matrix element eliminates the geometry from the problem and is the essential step that permits us to use a two-state approximation for the shielding. Previous calculations [34] of cross section saturation due to intense light interactions for repulsive curve crossings for room temperature conditions indicate that such an approximation should be adequate for our present purposes. Although we can expect to get a reasonable qualitative description of the physics of shielding, getting the quantitative details of saturation correct will require a full multichannel quantum treatment of the three-dimensional problem.

The wave packet has a momentum distribution $W(p,t)$, which can be obtained from Ψ with a Fourier transform ($\mathcal{F}$) with respect to R,

$$W(p,t) = |\mathcal{F}_R[\Psi(R,t)]|^2 . \tag{6}$$

Changes in the kinetic energy of the system can be seen as changes in $W(p,t)$ via the relation

$$E_{\text{kin}} = \frac{p^2}{2\mu} \equiv k_B\tilde{T}. \tag{7}$$

The latter relation connects the kinetic energy of the relative motion with effective temperature $\tilde{T}$.

The calculation of the shielding measure with wave packet dynamics is straightforward. We place the initial ($t = 0$) Gaussian wave packet $P_g(R,0) = |\Psi_g(R,0)|^2$ at some appropriate distance that is much larger than R_C. Then, using Eq. (1) we propagate the wave packet until $t = T$. The wave packet is given a negative initial momentum so that it moves towards smaller values of R and eventually reaches the interaction region near R_C. The propagation time T is chosen such that the shielding process is clearly over at the end of the calculation. The portion of the wave packet that remained on the ground state and reached eventually $R = 0$ gives the shielding measure P_S directly. Similarly we can determine the ground- and excited-state components of the wave packet that eventually returned to large distances. Fourier transforms of these components provide the energy exchange information [Eq. (6)].

Wave packet dynamics is limited by the Heisenberg uncertainty principle. For our studies we need a wave packet that at least initially is relatively well localized (ΔR small), but does not spread too fast (Δp small) and has a well-defined absolute initial mean momentum p_0 ($\Delta p/p_0 \ll 1$) which we can relate to the temperature $\tilde{T}$ using Eq. (7). For the Gaussian minimum uncertainty wave packet $\Delta R\Delta p = \hbar/2$, so we can obtain the above situation only approximately. If we express the momentum p in units of the laser photon momentum $\hbar k_0$ (the recoil momentum), and the distance R in units of $\lambda = 1/k_0$, then the spatial and momentum widths of the Gaussian wave packet are related by $\Delta R = 1/(2\Delta p)$.

The shielding measure, as well as the probability for excited-state production, can also be calculated using the standard quantum close-coupling method [28], in which one solves the time-independent Schrödinger equation with the Hamiltonian H from Eq. (2) using appropriate asymptotic boundary conditions,

$$H\Psi(R,E) = E\Psi(R,E). \tag{8}$$

Additional insights about the shielding process are provided by the close-coupling method, since solving Eq. (8) provides the full scattering matrix S for the problem in the absence of decay, and can also handle with relative ease both the ingoing and outcoming probability fluxes simultaneously. The S matrix is calculated for a single collision energy E, and must be averaged over the distribution of E for a particular experiment. The heating due to the process discussed in Sec. I that produces excited-state atoms is proportional to the probability of excited-state production, $|S_{ge}(E,I)|^2$.

Reference [28] used the close-coupled method to calculate trap loss probabilities due to exciting an attractive excited-state potential for the case of red detuning from resonance. This was done in a three-channel calculation containing the ground-state g, the attractive excited state e, and an extra artificial channel a. The potential for the artificial channel was selected to cross the excited-state potential at small internuclear separation R_a, where it could serve as a probe of the scattering current reaching this small distance on the excited state. Similarly, our present close-coupled calculation uses three channels: the ground state g, the repulsive excited state e, and an artificial probe channel a. In this case, the artificial potential is chosen to cross the ground-state potential at small R_a, characteristic of the inner zone process that is being suppressed. The matrix element $|S_{ga}(E,I)|^2$ measures the probability of starting with unit probability on the ground entrance channel and ending on the probe exit channel. Therefore, the shielding measure for light intensity I is given by the ratio

$$P_S = \frac{|S_{ga}(E,I)|^2}{|S_{ga}(E,I=0)|^2}. \tag{9}$$

This quantity is independent of the specific form of the artificial channel and the magnitude of the g-a coupling. Equation (9) was used to calculate the shielding measure shown in Ref. [16].

B. The semiclassical Landau-Zener approach

In the semiclassical approach one can ignore the Heisenberg uncertainty principle, and assume a well localized ($\Delta R = 0$) initial wave packet with $W(p,0) = \delta(p - p_0)$. This bridges the gap between the time-dependent and time-independent scattering theory by introducing a single initial momentum and hence a single energy wave packet. The next step is then to assume that this wave packet follows classical trajectories: its motion on each state (a) takes place under the force exerted by the potential curve of that particular state and (b) obeys the laws of Newton.

When the wave packet reaches the curve crossing at R_C and passes it with the momentum p, part of it will enter the excited state and the rest will remain on the ground state. The semiclassical approach is simple: we assume that the interaction region where the potential curves are strongly coupled ($|U_e - U_g| \lesssim \hbar\Omega/2$) is narrow and inside it the potential surfaces can be replaced by their tangents at R_C, see Fig. 2. Then we assume that the wave packet moves through this region with a constant momentum p and any acceleration on either potential curve remains negligible during this passage. Under these conditions the classical trajectory becomes simply $dR/dt = p/\mu$, and we can put it into the Landau-Zener model [23,24] to replace the linear time dependence in the energy level structure with linear spatial dependence. According to this model the excited portion of a wave packet going through such a linear level crossing is [29–31]

$$P_e = 1 - \exp\left(-\frac{2\pi\hbar\Omega^2}{\alpha|p|/\mu}\right), \tag{10}$$

where

$$\alpha = \left|\frac{\partial[U_e(R) - U_g(R)]}{\partial R}\right|_{R=R_C}. \tag{11}$$

The shielding is, in this case, only partial as the probability to reach the inner region is

$$P_g = 1 - P_e = \exp\left(-\frac{2\pi\hbar\Omega^2}{\alpha|p|/\mu}\right). \tag{12}$$

Hence in the absence of spontaneous decay the shielding measure P_S is equal to P_g. Usually for quantal wave packets with nonzero Δp one should average P_g and P_e over the initial momentum distribution $W(p,0)$ as discussed in Refs. [26,31].

After the excited-state component of the wave packet has been reflected, it passes the curve crossing for a second time. We can again apply the Landau-Zener approach for the stimulated population transfer back to the ground-state. Then we have a probability P_∞ to remain on the excited-state asymptotically,

$$P_\infty = P_e(1 - P_e). \tag{13}$$

This is the probability for the two atoms to emerge from the collision with the shared increase of kinetic energy equal to ΔE_∞ as explained in Sec. I. Of course, components that remained on the ground state and got eventually reflected can also contribute to P_∞, which leads to an increase of P_∞ by a factor of 2; we shall discuss this later in this article when we present some results. The quantum close-coupling method calculates $P_\infty = |S_{ge}(E,I)|^2$, which includes the contributions from both the direct and reflected paths and their interferences.

Certain conditions of validity need to be satisfied when the Landau-Zener approach is used. If the turning point for the incoming wave packet on the excited-state potential curve is within the interaction region around R_C ($E^0_{\rm kin} \lesssim \hbar\Omega/2$) the linearization of the classical trajectory ($dR/dt = \text{const}$) breaks down. Such situations have been analyzed in the collision literature [36–39] with great care. The spatial linearization can be violated especially for strong fields and small detunings, as the ground and excited states can remain coupled even for large R. In the original Landau-Zener theory the initial and final states are defined as asymptotically decoupled; this requirement is usually fulfilled automatically when both the spatial and temporal linearization conditions apply. These restrictions imply that the semiclassical picture is good only for weak fields (small Ω) and for high-energy collisions (large p), in which case the shielding is negligible, as Eq. (12) shows. However, our experience is that the above restrictions can be softened to some extent, allowing a reasonable description of the process with the Landau-Zener theory even for low energies, small detunings and strong fields [26,27,29].

C. Results

Our choice of a model system was initially motivated by the experiment of Ref. [21] in a sodium magneto-optical trap. In one configuration a probe laser was absorbed during the collision of two ground-state sodium ^2S atoms in their $F = 2$ hyperfine substate. Absorption of the probe photon caused the appearance of an ionization signal due to the presence of a second photoionization laser. It was found that the ionization signal disappeared when a cooling laser was present and tuned 10 MHz to the red of the $^2S(F = 2) \rightarrow {}^2P_{3/2}(F = 3)$ transition. This observation could be explained if shielding is provided when the cooling laser excites a repulsive molecular hyperfine state correlating with $^2S(F = 2) + {}^2P_{3/2}(F = 3)$ separated atoms. The cooling laser is tuned 50 MHz to the *blue* of this lower separated atom asymptote. Calculations of the Na_2 molecular hyperfine potentials show that such repulsive potential curves exist [22].

More recent experiments on trapped sodium have demonstrated the existence of shielding at $\Delta/2\pi \simeq 600$ MHz blue detuning with an observed magnitude of shielding measure that is consistent with our calculations [16]. As we shall show below, spontaneous decay has little effect at such large values of Δ. Our model calculations for

the much smaller detuning of 50 MHz provide a much more stringent test of the dynamical effects of excited-state spontaneous decay. We have chosen as a study case a sodium system with initial relative kinetic energy $E_{\rm kin}/k_B = 250\ \mu$K. This corresponds to $p_0 = 10\hbar k_0$. The wavelength of the atomic cooling transition is $\lambda = 589$ nm, so $k_0 = 1.067 \times 10^7\ {\rm m}^{-1}$. When expressed in recoil units, the momentum p gives the kinetic energy: $E_{\rm kin}/k_B = p^2 \times 2.5\ \mu$K. The excited-state potential curve in the crossing picture is

$$U_e(R) = \frac{C_3}{R^3} - \hbar\Delta. \tag{14}$$

The parameters are $C_3 = 10(ea_0)^2$ in atomic units and $\Delta/2\pi = 50$ MHz (equal to 5 atomic linewidths). For this choice, $R_C \simeq 1100\ a_0$, where $a_0 = 5.29 \times 10^{-11}$ m is the Bohr radius and e is the electron charge. The coupling between the levels is simply $\hbar\Omega$, where we take the Rabi frequency $\Omega/2\pi$ to be in the range 0–20 MHz. The flat ground state is assumed to have zero energy. The potential configuration is shown in Fig. 2. With Eq. (14) we have then

$$\alpha = 3\left(\frac{(\hbar\Delta)^4}{C_3}\right)^{1/3}. \tag{15}$$

For the quantum close-coupling calculation we have used

$$U_g(R) = \beta\left[\left(\frac{R_g}{R}\right)^{12} - \left(\frac{R_g}{R}\right)^{6}\right], \tag{16}$$

where $\beta = 4\times10^4\ {\rm cm}^{-1}$ and $R_g = 4.49a_0$ in atomic units, in order to produce a realistic inner turning point for the ground state.

In Fig. 3 we see that the shielding measure provided by wave packet dynamics (WPD), the quantum close-coupling method (QMCC) and the Landau-Zener approach (LZ) with and without average over the momentum distribution $W(p,0)$ agree reasonably well even for large Ω, where the linearization arguments are assumed to break down ($E_{\rm kin}$ of 250 μK corresponds to $\Omega/2\pi = 5$ MHz). One has to use the logarithmic scale in order to see any differences between the various results. This is just an example of how versatile the Landau-Zener approach is, despite the validity conditions that arise from quite legitimate physical arguments based on the original derivation of the time-dependent model. The proximity of the two Landau-Zener curves in Fig. 3 suggest that our initial wave packet with $p_0 = 10\hbar k_0$ and $\Delta p = 2\hbar k_0$ is a reasonable approximation for a single momentum state. In a wave packet with large $\Delta p/p_0$ one expects the Landau-Zener excitation probability P_e to favor the slower components, and then the average $\langle P_S\rangle_p = \langle P_g(p)W(p,0)\rangle_p$ should differ from $P_g(p_0)$ [31].

The shielding becomes complete as $P_g \to 0$ and the shielding-induced kinetic-energy exchange vanishes as $P_\infty \to 0$ (because $P_e \to 1$ and the stimulated population transfer back to the ground state becomes complete). This is where the main practical problem for shielding steps in. As Eqs. (10) and (15) predict, with large detunings the field intensity I needed for complete shielding is large ($\Omega \propto \sqrt{I}$). However, if we decrease the detuning too much, the blue-detuned laser starts to interfere with the cooling process itself. Moreover, the role of spontaneous decay increases as the detuning decreases, as the time it takes to reflect the wave packet increases with decreasing α (see the discussion in subsection III A). In the experiment of Ref. [21] this problem does not arise since the cooling laser itself provides the shielding effect.

Our standard shielding picture becomes a bit different if we allow the escaped component P_S to return after being reflected at the inner region R. This may happen if the transition at R_C is not saturated (weak field), i.e., $P_g \neq 0$. The returning ground-state component can interfere at R_C with the reflected excited-state component after the latter has partly returned to the ground state at R_C by stimulated population transfer. As a result one has to add a phase factor $P_\phi = 4\sin^2(\phi)$ into P_∞ in Eq. (13). The phase ϕ depends on the potential structure and Rabi coupling Ω as described, e.g., in Refs. [40,41] (this process is well studied in the literature for slow atomic collisions [39,42–45] and, therefore, we shall not dwell too much on the subject). Occasionally this double crossing model is also called the Landau-Zener model, although the term Landau-Zener-Stückelberg model is more appropriate (the phase term P_ϕ is the origin of the Stückelberg oscillations [46]). In Fig. 4 we show using the quantum close-coupling method how these oscillations modify P_∞. However, thermal and field averages are usually assumed to wipe out such phase effects, and then $P_\infty = \langle 4P_e(1-P_e)\sin^2(\phi)\rangle \simeq 2P_e(1-P_e)$, i.e., the two wave packet components can be added incoherently. It is sometimes possible to observe experimentally

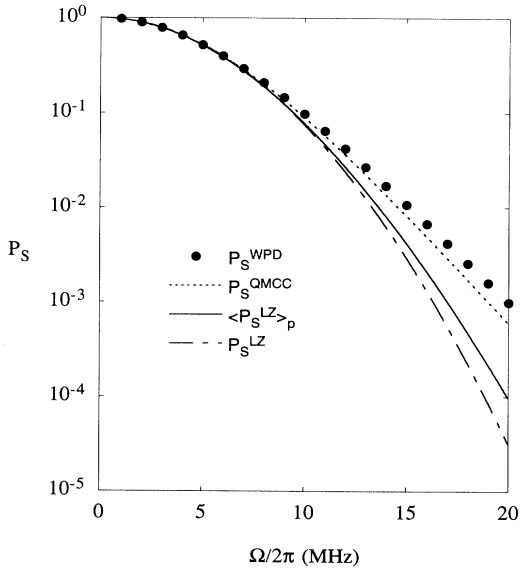

FIG. 3. The shielding measure P_S for weak spontaneous decay as a function of the Rabi coupling for Na atom collisions at 250 μK for a blue detuning of 50 MHz. We show the results from wave packet dynamics (WPD), quantum-mechanical close coupling (QMCC), and the Landau-Zener (LZ) model with and without averaging over the initial momentum distribution.

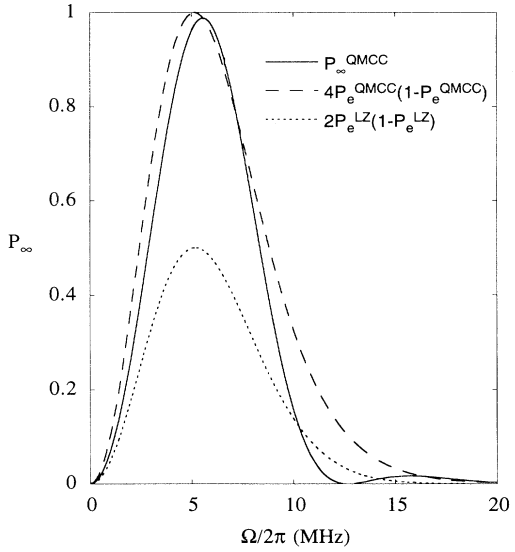

FIG. 4. The large R excited-state population P_∞ in the weak spontaneous decay case. We show the quantum close-coupling calculation result (P_∞^{QMCC}), the incoherent Landau-Zener prediction $2P_e^{\mathrm{LZ}}(1-P_e^{\mathrm{LZ}})$ from Eq. (13), and the assumed envelope $4P_e^{\mathrm{QMCC}}(1-P_e^{\mathrm{QMCC}})$ for the interference pattern, which is calculated from the QMCC result of Fig. 3.

the Stückelberg oscillations [47], but it is very difficult, and it remains an open question whether it is possible for cold collisions or not. The main point obtained from Fig. 4 is that even under the interference effect $P_\infty \to 0$ as we go to large intensities. Also, at the worst case the interference can only double P_∞ from the averaged value.

III. STRONG SPONTANEOUS DECAY

In this section we present some semiclassical estimates for the behavior of the shielding model in different parameter regions and extend the Landau-Zener model to include spontaneous decay when it cannot be ignored. A test for the model is provided by the quantum Monte Carlo method, which can also treat the energy exchange correctly.

A. Time scales and Landau-Zener models

The shielding process becomes complicated if spontaneous decay is present. As described in Sec. I and in Fig. 1(a) the excited-state wave packet can decay back to the ground state before it is reflected. The nature of spontaneous decay is global and temporal, so it is quite difficult to use time-independent descriptions for it except in the weak field limit. The parameter region where the semiclassical approach is justified is obtained by comparing the three characteristic time scales of our two-state shielding model. After the excitation of the wave packet the average time for the spontaneous decay to take place is

$$\tau_\gamma = \frac{1}{\gamma}, \tag{17}$$

where γ is the molecular decay parameter associated with the excited-state surface. In our study case the atomic decay parameter is $\gamma_{\mathrm{at}} = 1/(16\ \mathrm{ns})$, and we have taken $\gamma = 1.5\gamma_{\mathrm{at}}$.

In general we expect that the excited-state population is depleted as $\exp(-\gamma t)$, where t is the time spent on the excited state after the excitation at R_C. On the other hand, the time it takes for the wave packet to travel from R_C to R_{tp} is

$$\tau_{\mathrm{tp}} = \int_{R_C}^{R_{\mathrm{tp}}} \frac{dR'}{v(R',p)} = \int_{R_C}^{R_{\mathrm{tp}}} dR' \frac{\mu}{\sqrt{p_0^2 - 2\mu[U_e(R') - U_e(R_C)]}} \simeq \frac{|p_0|}{2\alpha}, \tag{18}$$

where $v(R')$ is the classical local velocity which depends on the initial momentum p_0 and the potential surface structure $U_e(R')$. The last expression is obtained by assuming that $-\alpha(R' - R_C)$ is a good approximate for $U_e(R')$ even at $R' = R_{\mathrm{tp}}$ (this should be quite true for our model as Fig. 2 suggests). The third time scale is the time it takes to traverse one half the interaction region,

$$\tau_\Omega \simeq \frac{\mu\hbar\Omega}{2\alpha|p_0|}. \tag{19}$$

If we compare Eqs. (18) and (19) we find that $\tau_{\mathrm{tp}} = \tau_\Omega$ when the wave packet is reflected at the inner edge of the interaction region, i.e., when $U_e(R_{\mathrm{tp}}) - U_e(R_C) = \hbar\Omega/2$. These time scales are crude approximations, but they can be used for discussing the role of spontaneous decay, and the role of recycling. It should be noted that τ_γ itself does not define whether the spontaneous decay is strong or not, but one has to compare it with the other two time scales. The relative ratios of these time scales can be used to establish six separate regions with their characteristic behaviors. These are summarized in Table I.

If τ_γ is large compared to both τ_{tp} and τ_Ω (regions I and II), spontaneous decay is weak and can be ignored during the shielding process. Then practically no decay occurs before the wave packet has been reflected. If also $\tau_{\mathrm{tp}} \gg \tau_\Omega$ (region I), which relation becomes $E_{\mathrm{kin}} \gg \hbar\Omega/2$, the temporal linearization argument is fulfilled and the Landau-Zener approach can be used safely, if also the linearization of the potential curves is valid. Otherwise the use of the Landau-Zener approach is dubious, since the wave packet can be strongly decelerated and even reflected before the excitation process is complete, and this may make P_e deviate from the Landau-Zener result of Eq. (10).

When $\tau_{\mathrm{tp}} \gg \tau_\gamma \gg \tau_\Omega$ (region III) the excitation and spontaneous decay processes clearly decouple. Then we can treat the excitation process with the Landau-Zener approach, and assume that afterwards the wave packet component on excited-state decays exponentially back to the ground state during its evolution. The shielding measure is, therefore, increased and we can estimate it with

TABLE I. The different cases in the semiclassical approach. The time scales appear in the order of decreasing length. The Landau-Zener theory is denoted by LZ and its extensions with LZD and LZDD.

Case	Relations	Description
I	$\tau_\gamma \gg \tau_{\rm tp} \gg \tau_\Omega$	no decay effect, LZ works
II	$\tau_\gamma \gg \tau_\Omega \gg \tau_{\rm tp}$	no decay effect, LZ dubious
III	$\tau_{\rm tp} \gg \tau_\gamma \gg \tau_\Omega$	no recycling, LZD works
IV	$\tau_{\rm tp} \gg \tau_\Omega \gg \tau_\gamma$	recycling present, LZDD works
V	$\tau_\Omega \gg \tau_{\rm tp} \gg \tau_\gamma$	recycling dominates, LZDD dubious
VI	$\tau_\Omega \gg \tau_\gamma \gg \tau_{\rm tp}$	no decay effect, LZ dubious

$$P_S = P_g + P_e[1 - \exp(-\gamma\tau_{\rm tp})] = 1 - P_e \exp(-\gamma\tau_{\rm tp}). \tag{20}$$

We call this a Landau-Zener model with decay (LZD), and it has been successfully employed in trap loss studies [28,48,49]. Since $\tau_\Omega \propto \Omega$, LZD is basically a weak field approach. We shall compare it with the quantum results in the subsection III C. For the experimental setup of Ref. [16] we have $1 - \exp(-\gamma\tau_{\rm tp}) \simeq 0.0213$, which obviously cannot cause any detectable deviation of P_S from P_g for any P_e.

If $\tau_{\rm tp} \gg \tau_\Omega \gg \tau_\gamma$ (region IV) then necessarily strong decay takes place within the interaction region, where the wave packet can be re-excited and the recycling becomes an important effect. Otherwise the basic validity conditions for the Landau-Zener theory are fulfilled. Results from our other studies [26,27] have suggested that in the presence of recycling the exponential decay starts only after the wave packet has reached the edge of the interaction region where recycling stops. Although the excitation process is clearly mixing with the decay in order to produce recycling, the Landau-Zener character of the process seems to prevail. Assuming that during the recycling the excited-state wave packet was also decelerated, we can update the LZD model of Eq. (20) to a LZDD model (Landau-Zener model with delayed decay):

$$P_S = 1 - P_e \exp(-\gamma\tau_{{\rm tp},\Omega}). \tag{21}$$

Here $\tau_{{\rm tp},\Omega} \equiv \tau_{\rm tp} - \tau_\Omega$ is simply the time it takes to move from the inner edge of the interaction region, located at

$$R_\Omega = \left(\frac{C_3}{\hbar\Delta + \hbar\Omega/2}\right)^{1/3}, \tag{22}$$

to the classical turning point $R_{\rm tp}$,

$$\tau_{{\rm tp},\Omega} = \int_{R_\Omega}^{R_{\rm tp}} dR' \, \frac{\mu}{\sqrt{p_0^2 - 2\mu[U_e(R') - U_e(R_\Omega)]}}, \tag{23}$$

where p_0 is the momentum of the wave packet at R_C. The above model clearly decreases the time for decay and hence increases the excited-state survival. This then leads to a decrease in the shielding measure P_S. For comparisons with wave packet results both Eqs. (20) and (21) can be averaged over $W(p,0)$ when needed.

For very strong fields τ_Ω is the largest time scale (regions V and VI). Then we have wave packet reflection and clear decay well within the interaction region. Some of the validity conditions for the Landau-Zener model are clearly violated, but as the studies for weak decay in Sec. II show, these conditions can be softened to some extent.

B. Dissipative wave packet dynamics

When the spontaneous decay is strongly present one has to solve the Liouville-von Neumann equation

$$i\hbar\frac{\partial\rho_{ij}(R,R')}{\partial t} = \sum_k [H_{ik}(R)\rho_{kj}(R,R') - \rho_{ik}(R,R')H_{kj}(R')] - i\hbar\sum_{kl}\Gamma_{ijkl}\rho_{kl}(R,R') \tag{24}$$

for the density matrix $\rho(R,R',t)$, instead of the Schrödinger equation (1). Here the Hamiltonian is the same as in Eq. (2), and the operator Γ represents the decay. Unfortunately, the problem cannot be treated by solving Eq. (24) because of limitations on current computers [33], although some limited studies can be made [31]. Hence we need an alternative method.

We apply the Monte Carlo wave function method, in the form derived in Ref. [32], to wave packet dynamics. Our numerical quantum approach has been discussed in detail in Refs. [26,33]. We add an optical potential to the system Hamiltonian H of Eq. (2) and solve the corresponding time-dependent Schrödinger equation (1) in one spatial dimension (R) only. Despite the optical potential the system remains closed, however, because after each time step the state vector (3) is renormalized to unity. The evolution process is disturbed by randomly selected quantum jumps which provide a unique wave packet history. This history is supposed to correspond to an observed evolution of a single system, with detection of the spontaneously emitted photons. A set of these histories are then combined into an ensemble that forms an adequate approximation to the full density matrix, i.e., the solution of Eq. (24).

In our shielding study the portion of the Monte Carlo wave packet that has reached $R = 0$ before the end of the integration, when $t = T$, is taken to correspond to P_S. Integration times T are chosen such that at $t = T$ we have wave packet components at $R \ll R_C$ and at $R \gg R_C$ only. The kinetic-energy exchange is determined by forming an ensemble of Fourier-transformed wave packets [Eq. (6)] alongside the ensemble for spatial evolution. Then we obtain $W(p,T)$ which can be matched against $W(p,0)$. Our model is a one-way study as we do not allow wave packet reflections at $R \simeq 0$, but otherwise determining P_S from wave packet studies would be difficult since ΔR tends to be large and the incoming components mix with the outgoing ones.

C. Results

We have tested the Landau-Zener approaches presented in Secs. II and III, i.e., Eqs. (12), (20), and (21).

The results for P_S are shown in Fig. 5. The solid line stands for the Landau-Zener prediction of Eq. (12), after a momentum average over $W(p,0)$. The solid circles show the results obtained with the Monte Carlo simulations, i.e., with decay. The dotted line is the LZD prediction of Eq. (20) with a momentum average. It saturates to the value $1-\exp(-\gamma\tau_{\rm tp})$ when $P_e \to 1$ (and $P_g \to 0$). The simulation results show that Eq. (20) works for roughly $\Omega \lesssim 2.5$ MHz, but then fails. However, the LZDD method of Eq. (21) with a momentum average (dashed line) gives a nice agreement with the simulation results.

The results confirm the assumptions we made when studying the time scales in the subsection III A. Interestingly, for $\Omega \gtrsim 10$ MHz we have $\tau_\Omega > \tau_{\rm tp}$ which means we are moving from region IV to region V, where the wave packet reflection takes place during recycling. But the LZDD model shows no indication of deviating from the wave packet results. The region of validity for LZD, i.e., region III, is very narrow for our particular study case, because $E^0_{\rm kin}$ is small. But there may be other systems where the validity conditions for Eq. (20) are fulfilled in a region where P_e is large. In any case the LZDD model converges to the LZD model in the weak field limit, so one can use LZDD in general. It is interesting to note that our model seems to work well for clearly nonzero widths of the interaction region, although we assume that the Landau-Zener excitation and the change from the ground-state classical trajectory to the excited-state classical trajectory takes place at a single point, namely $R = R_C$.

As mentioned before, the shielding produces an increase in kinetic energy as a side product. For weak spontaneous decay this is seen as a clear increase of $E_{\rm kin}$ equal to ΔE_∞. For strong decay, like in our study case, this increase is turned into a radiative heating, which disappears in the strong field limit. During the passage from R to $R \to \infty$ the excited-state wave packet decays exponentially, and the gain in kinetic energy sweeps over the local energy differences $U_e(R) - U_e(R \to \infty)$. This is seen in Fig. 6 where we show the momentum distributions $W_g(p,T)$ for the ground-state wave packet component at the end of the simulation ($t = T$). The part of the wave packet that has remained unshielded (P_S) has negative momentum, and the shielded part has positive momentum. We can see in each distribution a tail towards large positive momentum; these tails are clearly visible in the selected positive momentum close-ups of Fig. 7. They arise from the spontaneous decay at $R > R_C$, as mentioned earlier, and disappear when P_e becomes close to unity and the stimulated decay is practically complete. Then very little excited-state population survives to $R > R_C$ and contributes to the radiative energy exchange.

When considering the radiative heating one has to take into account the fact that decay takes place when the quasimolecule after reflection moves through the region between $R_{\rm tp}$ and R_C. Then we have decay-produced ground-state components with small positive momentum. They can either remain on the ground state or enter the excited state as they pass R_C. They may contribute to the lower end of the momentum distribution. However, this effect is not strong, as the peak positions in the close-ups shown in Fig. 7 are shifted only slightly below p_0. In our case the nonzero width of the wave packet masks this effect to some extent. The role of these decayed components may not necessarily be small for other systems, in which case they should be accounted for.

In the case of an attractive potential in our previous study [26], the recycling enhanced the kinetic-energy exchange and hence the heating associated with the shielding was large when $P_e \simeq 1$. However, in our shielding model the stimulated population transfer co-operates with spontaneous decay in shifting the reflected wave

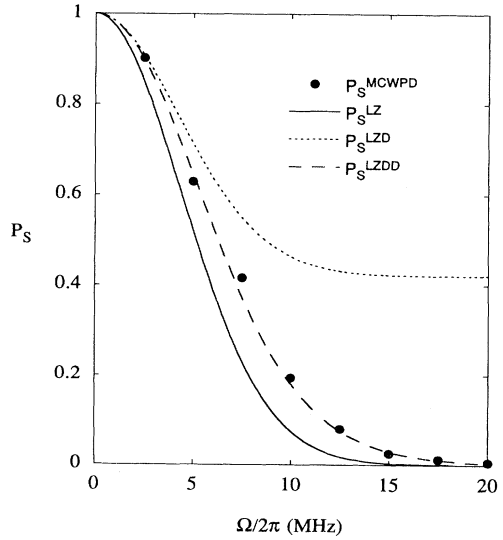

FIG. 5. The shielding measure P_S for strong spontaneous decay as a function of the Rabi coupling. The benchmark quantum results are from the Monte Carlo wave packet dynamics (MCWPD) calculations. Three different Landau-Zener models are applied (LZ, LZD, and LZDD).

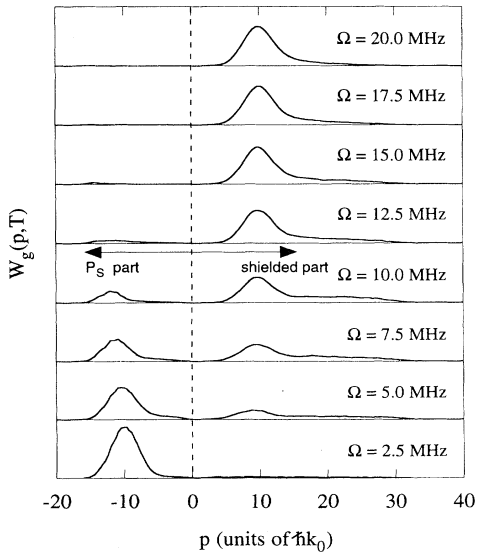

FIG. 6. The final ground-state wave packet momentum distributions. For brevity the 2π factor has been dropped from Ω in the curve labels.

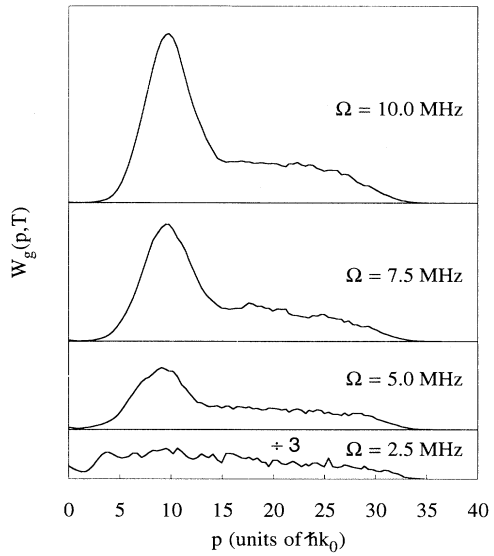

FIG. 7. The final ground-state wave packet momentum distributions for the shielded part. The radiative structure of kinetic-energy exchange produces the diffusive tails right of the main peak located near the initial momentum distribution, which is a Gaussian with $\langle p \rangle = 10\hbar k_0$ and $\Delta p = 2\hbar k_0$. For brevity the 2π factor has been dropped again from Ω in the curve labels.

packets back to the ground state. Hence there is no recycling effect which would force survival on the excited state at $R > R_C$, and the subsequent enhancement of kinetic-energy exchange is absent. Therefore, the shielding picture at large Ω with decay resembles very well the situation without decay and we can have complete elastic shielding in the presence of spontaneous decay.

IV. CONCLUSIONS

Our model for optical shielding follows from many simplifying assumptions and approximations. However, we believe that it contains some aspects that are also present in the actual experimental situation. In a wider perspective the surprising usefulness of the Landau-Zener model with and without spontaneous decay is very impressive. We would hope that this result would extend to the multichannel case needed to describe the alkali-atom and metastable rare-gas systems for which real experiments are being done. The model can be used as the basic tool for qualitative and even quantitative semiclassical description of processes related to cold collisions. This diminishes the need for time-consuming and tedious simulations, which in any case, because of the simplicity of the model, can in practice have only a qualitative role in comparisons with actual experiments. The key point in the use of the Landau-Zener model and its extensions is the time-dependent view of the process: the validity of semiclassical models can be determined by studying the relevant time scales. Our previous studies [25–28,31] support this approach to the cold collision problems.

With suitably strong fields one obtains, within the limits of our model, practically complete shielding, and simultaneously avoids the creation of additional heating or trap loss by the shielding process itself. This is due to the adiabatic nature of the excitation process and the recycling effect, upon which our semiclassical approach is based. The results from this approach are verified by the Monte Carlo simulation results surprisingly well. At large detunings, which is the usual case in experiments, the spontaneous decay can be ignored and the semiclassical description of shielding is reduced to the basic Landau-Zener model, which explicitly tells how the field detuning and intensity, and the trap temperature determine the excitation probability and hence the shielding efficiency. It should be pointed out, however, that we have not truly explored the region of strong saturation, which with large detunings is an unlikely situation to occur. In the presence of strong spontaneous decay and a laser coupling which can saturate the molecular transition even at large distances one can expect the recycling to turn into strong steady-state formation, which may well have an effect on the Landau-Zener view of the excitation process. Since such situations are more common in trap loss models, we are currently studying this particular parameter region (corresponding mainly to regions V and VI in Table I) in the context of attractive excited-state potentials. Also, for the shielding case one may then have to take into account the presence of other states, such as the attractive counterpart of the repulsive excited state used in this paper.

A complete quantum-mechanical treatment of the shielding process for realistic atoms must also take into account the role of atomic and molecular degeneracy and the selection rules for radiative transitions contained in Eq. (4). Even the simplest system for laser cooling, a $^1S \rightarrow {}^1P$ transition without nuclear or electron spin, such as provided by Ca or Mg atoms, has the possibility of $J' = J \pm 1$ transitions as well as a range of M projection quantum numbers. This is because a strong radiation field breaks the spherical symmetry of the field-free quasimolecular system, thereby giving rise to an infinite set of coupled Schrödinger equations instead of the two coupled ones in Eq. (8) [34]. In practice such equation sets can be truncated for very low energy collisions after a relatively few angular momenta are included in the hierarchy. For normal temperature collisions, solving a truncated set of equations leads to slower saturation with laser power I than predicted by two-state models of the type we have employed here. It is now important to construct more realistic quantum-mechanical models of shielding in the low T limit, in order to test the limitations of the two-state model.

Our purpose in this paper has not been to describe specific experiments but to develop some general concepts about the physics of optical shielding of collisions. We describe in a separate publication [16] the good agreement between quantum and LZ model calculations and the observed shielding in a Na magneto-optical trap at 600 MHz = 60 γ blue detuning. Another recent publication [17] also suggests that an LZ model can account for the experimentally observed saturation of repulsive state excitation in a Rb magneto-optical trap. On the other hand,

Ref. [19] has reported a saturation of shielding measure for Penning ionization collisions of trapped metastable $Xe(j = 2)$ atoms at a magnitude of $P_S \approx 0.2$ as the power of the shielding laser increased. This saturation limit corresponds to much less effective shielding than would be predicted by a two-level model. This discrepancy demonstrates the necessity of developing more realistic three-dimensional multichannel quantum-mechanical models of the shielding process. We are currently working on improved models. In any case, we expect that much of the qualitative physics contained in the two-state models will carry over to the general case, even if some revision of quantitative predictions concerning saturation should be necessary.

Finally, there is one other avenue that should be explored in the context of achieving the high atomic density and low temperature needed to achieve Bose-Einstein condensation. In addition to lowering the ground-state inelastic collision rate without necessarily introducing significant additional inelastic processes, the ground-state elastic scattering rate can be strongly increased by the strong radiative interactions at long range near R_C. This prospect could lead to improved evaporative cooling rates, if evaporative cooling proves to be a viable scheme for cooling species other than hydrogen [50]. A careful study of the low T behavior of the elastic scattering properties of the ground state in a shielding laser field needs to be carried out.

ACKNOWLEDGMENTS

This work has been supported by grants from the Office of Naval Research, the Army Research Office, the U.K. Engineering and Physical Sciences Research Council and the Academy of Finland. The authors wish to thank Carl Williams for helpful discussions. K.-A.S. thanks NIST for hospitality.

[1] P. S. Julienne, A. M. Smith, and K. Burnett, in *Advances in Atomic, Molecular and Optical Physics, Vol. 30*, edited by D. R. Bates and B. Bederson (Academic Press, San Diego, 1993), pp. 141–198.
[2] D. Sesko, T. Walker, C. Monroe, A. Gallagher, and C. Wieman, Phys. Rev. Lett. **63**, 961 (1989).
[3] A. Gallagher and D. E. Pritchard, Phys. Rev. Lett. **63**, 957 (1989).
[4] P. S. Julienne and J. Vigué, Phys. Rev. A **44**, 4464 (1991).
[5] C. D. Wallace, T. P. Dinneen, K.-Y. N. Tan, T. T. Grove, and P. L. Gould, Phys. Rev. Lett. **69**, 897 (1992).
[6] D. Hoffman, P. Feng, R. Williamson, and T. Walker, Phys. Rev. Lett. **69**, 753 (1992).
[7] L. Marcassa, V. Bagnato, Y. Wang, C. Tsao, J. Weiner, O. Dulieu, Y. B. Band, and P. S. Julienne, Phys. Rev. A **47**, R4563 (1993).
[8] J. Kawanake, K. Shimizu, H. Tanaka, and F. Shimizu, Phys. Rev. A **48**, R883 (1993).
[9] N. W. M. Ritchie, E. R. I. Abraham, Y. X. Xiao, C. C. Bradley, R. G. Hulet, and P. S. Julienne (unpublished).
[10] J. D. Miller, R. A. Cline, and D. J. Heinzen, Phys. Rev. Lett. **71**, 2204 (1993).
[11] R. A. Cline, J. D. Miller, and D. J. Heinzen, Phys. Rev. Lett. **73**, 632 (1994).
[12] H. T. C. Stoof, J. M. V. A. Koelman, and B. J. Verhaar, Phys. Rev. B **38**, 4688 (1988).
[13] E. Tiesinga, A. J. Moerdijk, B. J. Verhaar, and H. T. C. Stoof, Phys. Rev. A **46**, R1167 (1992).
[14] B. Verhaar, K. Gibble, and S. Chu, Phys. Rev. A **48**, R3429 (1993).
[15] Ch. Monroe, E. Cornell, and C. Wieman, in *Laser Manipulation of Atoms and Ions*, Proceedings of the International School of Physics "Enrico Fermi," Course CXVIII, Varenna, Italy, 1991, edited by E. Arimondo, W. D. Phillips, and F. Strumia (North-Holland, Amsterdam, 1992), pp. 361–377.
[16] L. Marcassa, S. Muniz, E. de Queiroz, S. Zilio, V. Bagnato, J. Weiner, P. S. Julienne, and K.-A. Suominen, Phys. Rev. Lett. **73**, 1911 (1994).
[17] S. Bali, D. Hoffman, and T. Walker, Europhys. Lett. **27**, 273 (1994).
[18] K. Y. N. Tan, S. D. Gensemer, C. D. Wallace, A. Kumarakrishnan, and P. L. Gould (unpublished).
[19] M. Walhout, U. Sterr, C. Orzel, M. Hoogerland, and S. Rolston, Phys. Rev. Lett. **74**, 506 (1995).
[20] H. Katori and F. Shimizu, Phys. Rev. Lett. **73**, 2555 (1994).
[21] V. Bagnato, L. Marcassa, C. Tsao, Y. Wang, and J. Weiner, Phys. Rev. Lett. **70**, 3225 (1993).
[22] C. J. Williams and P. S. Julienne, J. Chem Phys. **101**, 2634 (1994).
[23] L. D. Landau, Phys. Z. Sowjetunion **2**, 46 (1932).
[24] C. Zener, Proc. R. Soc. London Ser. A **137**, 696 (1932).
[25] M. J. Holland, K.-A. Suominen, and K. Burnett, Phys. Rev. Lett. **72**, 2367 (1994).
[26] M. J. Holland, K.-A. Suominen, and K. Burnett, Phys. Rev. A **50**, 1513 (1994).
[27] Y. B. Band, I. Tuvi, K.-A. Suominen, K. Burnett, and P. S. Julienne, Phys. Rev. A **50**, 2826 (1994).
[28] P. S. Julienne, K.-A. Suominen, and Y. B. Band, Phys. Rev. A **49**, 3890 (1994).
[29] B. M. Garraway and S. Stenholm, Opt. Commun. **83**, 349 (1991).
[30] B. M. Garraway, S. Stenholm, and K.-A. Suominen, Phys. World **6**, 46 (1993).
[31] K.-A. Suominen and B. M. Garraway, Phys. Rev. A **48**, 3811 (1993).
[32] J. Dalibard, Y. Castin, and K. Mølmer, Phys. Rev. Lett. **68**, 580 (1992); Y. Castin, K. Mølmer, and J. Dalibard, J. Opt. Soc. Am. B **10**, 524 (1993).
[33] W. K. Lai, K.-A. Suominen, B. M. Garraway, and S. Stenholm, Phys. Rev. A **47**, 4779 (1993).
[34] P. S. Julienne and F. H. Mies, Phys. Rev. A **25**, 3399 (1982).
[35] P. L. Devries and T. F. George, Mol. Phys. **36**, 151 (1978); *ibid.* **38**, 561 (1979); Phys. Rev. A **18**, 1751 (1978).
[36] E. E. Nikitin, Opt. Spectrosc. **11**, 246 (1961).
[37] M. Ya. Ovchinnikova, Opt. Spectrosc. **17**, 447 (1964).

[38] V. K. Bykhovskii, E. E. Nikitin, and M. Ya. Ovchinnikova, Zh. Eksp. Teor. Fiz. **47**, 750 (1964) [Sov. Phys. JETP **20**, 500 (1965)].
[39] E. E. Nikitin and S. Ya. Umanskii, *Theory of Slow Atomic Collisions* (Springer-Verlag, Berlin, 1984).
[40] A. Bárány and D. S. F. Crothers, Phys. Scr. **23**, 1096 (1981).
[41] B. M. Garraway and S. Stenholm, Phys. Rev. A **46**, 1413 (1992).
[42] E. E. Nikitin and A. I. Reznikov, Phys. Rev. A **6**, 522 (1972).
[43] M. S. Child, *Molecular Collision Theory* (Academic Press, London, 1974).
[44] B. C. Eu, *Semiclassical Theories of Molecular Scattering* (Springer-Verlag, Berlin, 1984).
[45] M. S. Child, *Semiclassical Mechanics with Molecular Applications* (Clarendon Press, Oxford, 1991).
[46] E. C. G. Stückelberg, Helv. Phys. Acta **5**, 369 (1932).
[47] S. Yoakum, L. Sirko, and P. M. Koch, Phys. Rev. Lett. **69**, 1919 (1992).
[48] K.-A. Suominen, M. J. Holland, K. Burnett, and P. S. Julienne, Phys. Rev. A **49**, 3897 (1994).
[49] H. M. J. M. Boesten and B. J. Verhaar, Phys. Rev. A **49**, 4240 (1994).
[50] J. Doyle, J. Sandberg, I. Yu, C. Cesar, D. Kleppner, and T. Greytak, Phys. Rev. Lett. **67**, 603 (1991).